

# Membrane imaging by simultaneous second-harmonic generation and two-photon microscopy

L. Moreaux

*Laboratoire de Physiologie, Ecole Supérieure de Physique et Chimie Industrielles,  
Institut National de la Santé et de la Recherche Médicale, Equipe Postulante 00-02, 10 rue Vauquelin, 75005 Paris, France*

O. Sandre

*Laboratoire Physico-Chimie Curie, Centre National de la Recherche Scientifique, Unité Mixte de Recherche 168,  
11 rue Pierre et Marie Curie, 75005 Paris, France*

M. Blanchard-Desce

*Département de Chimie, Ecole Normale Supérieure, Centre National de la Recherche Scientifique,  
Unité Mixte de Recherche 8640, 24 rue Lhomond, 75005 Paris, France*

J. Mertz

*Laboratoire de Physiologie, Ecole Supérieure de Physique et Chimie Industrielles,  
Institut National de la Santé et de la Recherche Médicale, Equipe Postulante 00-02, 10 rue Vauquelin, 75005 Paris, France*

Received October 20, 1999

We demonstrate that simultaneous second-harmonic generation (SHG) and two-photon-excited fluorescence (TPEF) can be used to rapidly image biological membranes labeled with a styryl dye. **The SHG power is made compatible with the TPEF power by use of near-resonance excitation**, in accord with a model based on the theory of phased-array antennas, which shows that the SHG radiation is highly structured. Because of its sensitivity to local asymmetry, SHG microscopy promises to be a powerful tool for the study of membrane dynamics. © 2000 Optical Society of America

OCIS codes: 190.4160, 190.4180, 180.5810, 170.5810, 190.4350, 190.4710.

Second-harmonic generation (SHG) and two-photon-excited fluorescence (TPEF) are nonlinear optical phenomena that scale with the square of excitation intensity and hence give rise to the same intrinsic three-dimensional resolution when they are used in microscopic imaging. Whereas TPEF microscopy has now become a laboratory standard,<sup>1</sup> SHG microscopy at high resolution has only recently been demonstrated as a tool for imaging nonlinear susceptibilities of inorganic or organic materials<sup>2,3</sup> and of molecular probes specifically designed to report membrane potential.<sup>4,5</sup> Because SHG is a coherent phenomenon that involves radiative scattering whereas TPEF is an incoherent phenomenon that involves radiative absorption and reemission, the two provide intrinsically different contrasts. We study here the possibility of combining these contrasts in a single microscope. In most cases, molecular SHG has been demonstrated far off resonance, resulting in little absorption but also in low SHG efficiency even for large static hyperpolarizabilities. As a result, high excitation powers and long integration times become necessary, which are incompatible with most biological TPEF microscopy. By using a charge transfer donor-( $\pi$ -bridge)-acceptor styryl dye<sup>6,7</sup> and exciting near (above) the absorption band, we benefit from a ten- to hundred-fold increase in SHG signal and also a significant two-photon absorption. We show that this enhancement in SHG efficiency along with the coherent summation of field amplitudes results in large SHG power, which permits simultaneous and rapid SHG and TPEF imaging of bio-

logical membranes. Moreover, the SHG radiation is found to be symmetrically peaked in two well-defined directions. We demonstrate finally that SHG and TPEF provide complementary information about the organization of the dye in a membrane.

Our experimental layout is described in Fig. 1 and consists of a home-built TPEF microscope that includes

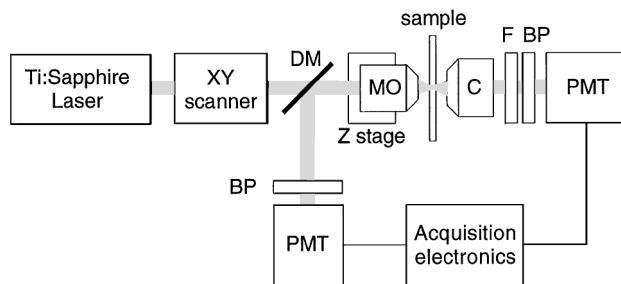


Fig. 1. Experimental layout: Ti:sapphire laser light is focused into a sample with a microscope objective (MO; 0.9-N.A. water immersion; Olympus). The transmitted SHG is collected with a condenser (C; 1.4-N.A., Olympus), bandpass (BP) filtered, and detected with a photomultiplier tube (PMT). The transmitted laser light is blocked with a  $\text{CuSO}_4$  colored-glass filter (F). The TPEF from the sample is epicollected, discriminated with a dichroic mirror (DM), bandpass (BP) filtered, and detected with a PMT. Three-dimensional images are formed by scanning of the laser focal spot in the XY directions with galvanometer-mounted mirrors and in the Z direction by translation of the microscope objective.

detection of transmitted light. The excitation source is a mode-locked Ti:sapphire laser (Coherent), which delivers  $\sim 120$ -fs pulses at a 76-MHz repetition rate. The laser light is focused into the sample, and the resultant SHG is collected in the forward direction while the TPEF is collected in the backward direction. The sample consists of giant unilamellar vesicles made from a phospholipid in water. The vesicles are labeled at 1 mol.% with the lipophilic styryl dye *N*-(4-sulfobutyl)-4-(4-(dihexylamino)styryl)pyridinium (Di-6-ASPBS); preparation and labeling are described elsewhere.<sup>8</sup> When the dye is inserted into a membrane, its charge-transfer axis lies perpendicular to the membrane plane, as confirmed by polarization analysis, and the radiative absorption and fluorescence maxima are at 465 and 575 nm, respectively.<sup>9</sup> We denote as  $\beta$  the dye hyperpolarizability along its charge-transfer axis.<sup>10,11</sup>

When a tightly focused excitation beam is used in TPEF microscopy, the active volume from which fluorescence is generated is sharply confined near the focal center. Similarly, when one is imaging molecules in a membrane with SHG microscopy, only a small area about the focal center is active. Given the length scales involved, this area may be considered essentially flat and oriented parallel to the excitation propagation direction, as shown in Fig. 2. This differs from the usual geometry used for studying surface SHG by specular reflection of an unfocused excitation beam.<sup>12</sup> We therefore have developed a model specifically tailored to our geometry to characterize SHG in a membrane. Our model is derived from the theory of phase-array antennas, in which the dye molecules are regarded as elemental dipole radiators driven at the second-harmonic frequency of the excitation beam, in proportion to their hyperpolarizability. To an excellent approximation, the focused excitation beam amplitude may be considered to have Gaussian profiles in the lateral and axial directions, with waists  $w_x$  and  $w_z$ , respectively. A property of a focused beam is that, while its phase varies linearly along the propagation direction  $z$  about the focal center, this phase is retarded relative to the corresponding phase of an unfocused plane wave (an effect often referred to as a phase anomaly). The effective wave vector of the focused beam near its focal center can then be written as  $\xi k_w$ , where  $\xi$  is less than 1 and  $k_w$  is the wave vector of an unfocused beam. In our case,  $w_x = 510$  nm,  $w_z = 1.9$   $\mu$ m, and  $\xi$  is numerically evaluated to be  $\sim 0.87$  [for weakly focused beams,  $\xi$  may be roughly approximated by  $1 - 2/(k_w w_x)^2$ ]. By taking the excitation polarization to be along the charge-transfer axis  $y$  and coherently summing the far-field amplitudes produced by the radiating dye molecules, we can then derive the SHG power per differential solid angle:

$$P_{2\omega}(\theta, \varphi) = \frac{\omega^4}{2\pi^2 n \epsilon_0^3 c^5} N^2 \beta^2 S(\theta, \varphi) I_\omega^2, \quad (1)$$

where  $\omega$  is the excitation frequency,  $n$  is the index of refraction (we assume that  $n_\omega \approx n_{2\omega}$  and neglect local-field factors),  $N = \pi N_s w_x w_z / 2$  is the effective number of molecules that contribute to SHG, and  $S(\theta, \varphi)$  is the

angular radiation distribution (see Fig. 2). The structure of  $S(\theta, \varphi)$  critically depends on  $\xi$  and exhibits two symmetric peaks, at  $\theta_{\text{peak}} = \pm \cos^{-1}(\xi)$ , corresponding to the angles where the excitation and SHG fields are phase matched. The total SHG power,  $P_{\text{SHG}}$ , is obtained by integration of Eq. (1) over all solid angles. Although the expression for this power can be evaluated only numerically, we can estimate it by making use of small-angle approximations about  $\pm \theta_{\text{peak}}$ , obtaining

$$\Theta = \int \frac{3}{8\pi} S(\theta, \varphi) d\Omega \approx \frac{3\pi\xi^2}{4k_w^2 w_x w_z \sqrt{1-\xi^2}}. \quad (2)$$

To compare SHG and TPEF powers we use Eq. (1) to define a SHG cross section for a single molecule:

$$\sigma_{\text{SHG}} = \frac{4\hbar\omega^5}{3\pi^2 n \epsilon_0^3 c^5} \beta^2 \quad [\text{m}^4/\text{photon s}^{-1}], \quad (3)$$

which leads to a simple expression for the ratio of total SHG to TPEF powers:

$$\frac{P_{\text{SHG}}}{P_{\text{TPEF}}} \approx \Theta \frac{N \sigma_{\text{SHG}}}{\sigma_{\text{TPEF}}}. \quad (4)$$

The hyperpolarizabilities of organic nonlinear molecules are typically measured by experiments that involve electric-field-induced second-harmonic generation and hyper-Rayleigh scattering.<sup>10</sup> Although no direct experimental data on the hyperpolarizability of styryl dyes in membrane are available, the hyperpolarizability component along the charge-transfer axis for these molecules has been found to be well described by perturbation theory with a two-state model.<sup>10,11</sup> By including damping in this model<sup>12</sup> and based on electrochromism measurements for similar dyes in membranes,<sup>9</sup> we can predict a large near-resonance hyperpolarizability of approximately

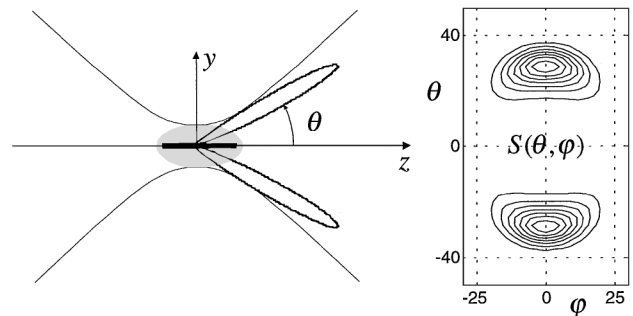


Fig. 2. Left, an excitation beam propagating in the  $z$  direction and polarized along the  $y$  axis is focused (side-on) onto the membrane of a labeled lipid vesicle. Only a small surface area (thick segment; side view) of this much larger vesicle contributes to SHG. The surface area is defined by  $N/N_s$ , where  $N$  is the effective number of radiating molecules and  $N_s$  is their surface density (molecules/unit membrane area). Right, the SHG radiation is double peaked in the forward direction with a far-field power distribution given by  $S(\theta, \varphi)$ . The peaks are separated in the  $y$ - $z$  plane by  $2\theta_{\text{peak}} \approx 60^\circ$ .

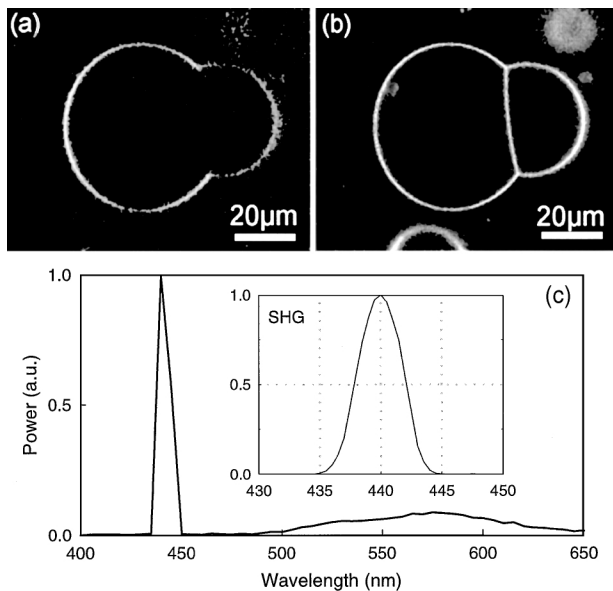


Fig. 3. (a) SHG and (b) TPEF images of two adhering vesicles labeled with Di-6-ASPBS (equatorial slice), excited at 880 nm. The total acquisition time for the images was 1.5 s, for an excitation power at the sample of  $<1$  mW. The adhesion area where the membranes are fused exhibits a centrosymmetric molecular distribution wherein TPEF is allowed but SHG is not. The corresponding forward-detected emission spectra of SHG (left peak) and TPEF (right peak) are shown in (c). The large Stokes shift in fluorescence gives rise to a large spectral separation between the two emission peaks. An expanded view of the SHG peak is shown in the inset (4-nm resolution).

$\beta \approx 1 \times 10^{-47} \text{ C m}^3 \text{ V}^{-2}$  for Di-6-ASPBS at an 880-nm excitation wavelength or, equivalently,  $\sigma_{\text{SHG}} \approx 1 \times 10^{-3} \text{ GM}$  ( $1 \text{ GM} = 10^{-50} \text{ cm}^4/\text{photon s}^{-1}$ ). In turn, the TPEF cross section of Di-6-ASPBS in a membrane at the same excitation wavelength is estimated to be  $\sigma_{\text{TPEF}} \approx 30 \text{ GM}$  (based on a TPEF measurement in ethanol). Although  $\sigma_{\text{SHG}}$  is small compared with  $\sigma_{\text{TPEF}}$  for a single molecule, the ratio  $P_{\text{SHG}}/P_{\text{TPEF}}$  is significantly enhanced for a large number of molecules owing to the coherent summation of SHG field amplitudes. In our case  $N_s = 1.5 \times 10^{16} \text{ m}^{-2}$ , and this ratio approaches 0.1. This ratio is even further enhanced if we consider that SHG power, because of its directional nature, can be more efficiently collected than TPEF power. In particular, an evaluation of  $S(\theta, \varphi)$  shows that in general essentially all the SHG power can be collected by a condenser N.A. that is equal to the excitation N.A. In contrast, only  $\sim 20\%$  of the TPEF power is collected by our epicollection N.A. of 0.9. We confirmed that  $S(\theta, \varphi)$  is double peaked by using both variable-aperture and slit detection. We also point out that  $P_{\text{SHG}}$  and  $P_{\text{TPEF}}$  roughly scale as N.A. here,

meaning that their power ratio is roughly independent of N.A.

Figure 3 illustrates SHG and TPEF images of Di-6-ASPBS molecules under the conditions described above. Near-resonance excitation combined with the coherent summation of SHG resulted in approximately equal measured powers in both images, allowing both images to be acquired simultaneously. We emphasize that the measured powers were high enough that we could operate with integration times of only  $10 \mu\text{s}$  per pixel, meaning that both SHG and TPEF can be used here to probe relatively rapid membrane dynamics. A feature of SHG is that it is a sensitive monitor of local molecular asymmetry. In particular, it is well known that SHG vanishes in the case of symmetric dipole distributions, as illustrated in Fig. 3. This sensitivity to local asymmetry is inaccessible to TPEF and promises to be a powerful tool for the study of molecular dynamics in biological membranes, for example, during membrane fusion or internalization.

The authors thank the Institut Curie for financial support. This work was initiated while L. Moreaux and J. Mertz were associated with the Centre National de la Recherche Scientifique, Unité Mixte de Recherche-7637, to which L. Moreaux is grateful for a Bourse Docteur Ingénieur fellowship. J. Mertz's e-mail address is [jerome.mertz@espci.fr](mailto:jerome.mertz@espci.fr).

## References

1. W. Denk, J. H. Strickler, and W. W. Webb, *Science* **248**, 73 (1990).
2. R. Gauderon, P. B. Lukins, and C. J. R. Sheppard, *Opt. Lett.* **23**, 1209 (1998).
3. Y. Guo, P. P. Ho, H. Savage, D. Harris, P. Sacks, S. Schantz, F. Liu, N. Zhadin, and R. R. Alfano, *Opt. Lett.* **22**, 1323 (1997).
4. P. J. Campagnola, M. Wei, and L. M. Loew, *Biophys. J.* **76**, A95 (1999).
5. G. Peleg, A. Lewis, M. Linial, and L. M. Loew, *Proc. Natl. Acad. Sci. USA* **96**, 6700 (1999).
6. S. R. Marder, D. N. Beratan, and L.-T. Cheng, *Science* **252**, 103 (1991).
7. T. Kogej, D. Beljonne, F. Meyers, J. W. Perry, S. R. Marder, and J. L. Brédas, *Chem. Phys. Lett.* **298**, 1 (1998).
8. O. Sandre, L. Moreaux, and F. Brochard, *Proc. Natl. Acad. Sci. USA* **96**, 10,588 (1999).
9. L. M. Loew and L. L. Simpson, *Biophys. J.* **34**, 353 (1981).
10. D. S. Chemla and J. Zyss, eds., *Nonlinear Optical Properties of Organic Molecules and Crystals* (Academic, New York, 1984), Vol. 1.
11. J. L. Oudar and D. S. Chemla, *J. Chem. Phys.* **66**, 2664 (1977).
12. Y. R. Shen, *The Principles of Nonlinear Optics* (Wiley, New York, 1984).